Plasma Phys. Control. Fusion 37 (1995) A69–A85. Printed in the UK

Recent D-T Results on TFTR

D W Johnson, V Arunasalam, C W Barnes,[1] S H Batha,[2] G Bateman, M Beer, M G Bell, R Bell, M Bitter, N L Bretz, R Budny, C E Bush,[3] S Cauffman, C S Chang,[4] Z Chang, C Z Cheng, D S Darrow, R Dendy,[5] W Dorland,[6] H H Duong,[7] R Durst,[8] P C Efthimion, D Ernst,[9] H Evenson,[8] N Fisch, R Fisher,[7] R J Fonck,[6] E Fredrickson, G Y Fu, T Fujita,[10] H P Furth, N Gorelenkov,[11] B Grek, L R Grisham, G Hammett, R J Hawryluk, W Heidbrink,[12] H W Herrmann, K W Hill, J Hosea, H Hsuan, M Hughes,[13] A Janos, D L Jassby, F C Jobes, L C Johnson, J Kamperschroer, J Kesner,[9] M Kotschenreuther,[6] H Kugel, P H LaMarche, B LeBlanc, F M Levinton,[2] J Machuzak,[9] R Majeski, D K Mansfield, E S Marmar,[9] E Mazzucato, M Mauel,[14] J McChesney,[7] K M McGuire, G McKee,[8] D M Meade, S S Medley, D R Mikkelsen, S V Mirnov,[11] D Mueller, R Nazikian, M Osakabe,[15] D K Owens, H Park, W Park, P Parks,[8] S F Paul, M Petrov,[16] C K Phillips, M Phillips,[13] A L Qualls,[3] A Ramsey, M H Redi, G Rewoldt, D Roberts,[8] J Rogers, A L Roquemore, E Ruskov,[11] S A Sabbagh,[14] M Sasao,[15] G Schilling, J Schivell, G L Schmidt, S D Scott, I Semenov,[11] S Sesnic, C H Skinner, D Spong,[3] B C Stratton, J D Strachan, W Stodiek, E Synakowski, H Takahashi, W Tang, G Taylor, J Terry,[9] W Tighe, J R Timberlake, A von Halle, S von Goeler, R White, J R Wilson, K L Wong, G A Wurden,[1] K M Young, M C Zarnstorff, and S J Zweben

Plasma Physics Laboratory, Princeton University, Princeton, N J 08543 USA

[1]Los Alamos National Laboratory, Los Alamos, New Mexico

[2]Fusion Physics and Technology, Torrance, California

[3]Oak Ridge National Laboratory, Oak Ridge, Tennessee

[4]Courant Institute, New York University, New York, New York

[5]Culham Laboratory, Abingdon, UK

[6]University of Texas, Institute for Fusion Studies, Texas

[7]General Atomics, San Diego, California

[8]University of Wisconsin, Madison, Wisconsin

[9]Massachusetts Institute of Technology, Cambridge, Massachusetts

[10]JAERI Naka Fusion Research Establishment, Naka, Japan

[11]TRINITI, Moscow, Russia

[12]University of California, Irvine, California

[13]Grumman Corporation, Princeton, New Jersey

[14]Columbia University, New York, New York

[15]National Institute of Fusion Studies, Nagoya, Japan

[16]Ioffe Physical-Technical Institute, Russia

Abstract. Routine tritium operation in TFTR has permitted investigations of alpha particle physics in parameter ranges resembling those of a reactor core. ICRF wave physics in a DT plasma and the influence of isotopic mass on supershot confinement have also been studied. Continued progress has been made in optimizing fusion power production in TFTR, using extended machine capability and Li wall conditioning. Performance is currently limited by MHD stability. A new reversed magnetic shear regime is being investigated with reduced core transport and a higher predicted stability limit.

0741-3335/95/11A069+17$19.50

1. Introduction

The goal of many decades of world-wide fusion research, performed until recently in H and D plasmas, has been the DT burning reactor, sustained by alpha particle heating. Operation in mixed DT plasmas began with the limited objective experiments on JET in 1991 (JET Team 1992), which produced a peak fusion power of 1.7 MW. Over the last 1.5 years, TFTR has extended the fusion power performance to 10.7 MW, with up to 6.5 MJ fusion energy per pulse. At these levels, the fusion power density in the core, ~2 MW/m^3, as well as many alpha parameters are comparable to those expected for the core of ITER.

Extending fusion power performance on TFTR promotes studies of alpha particle physics. We report studies of alpha particle confinement and slowing down, and of the effects of sawteeth on the radial redistribution of alpha particles. Documentation of alpha particle first orbit loss is given, which agrees with modeling. We observe increased alpha particle losses which correlate with MHD, with fast wave ICRF heating, and with the onset of disruptions. The spatial profile and time evolution of alpha ash has been measured and modeled. Alpha driven TAE modes have not been observed, but there is evidence of the contribution of alpha particle drive in the destabilizion of RF-driven TAE modes, and edge localized alpha-driven ICE has been observed. Evidence for alpha particle heating of electrons is given.

The success of Li wall conditioning in improving supershot confinement has been dramatic. This technique has provided valuable flexibility in operating near the MHD stability limit, even at full machine parameters. However, continued improvement in the fusion power performance of supershots will require enhanced stability.

According to theory, current profile modification offers potential for improved stability. We describe initial experiments with a modified current profile characterized by a region of reversed magnetic shear, which exhibits enhanced core confinement characteristics, and is predicted to have improved stability.

2. Operating Experience with DT Plasmas

Since December 1993, over 400 discharges were fueled and heated with at least one neutral beam source using tritium. Mixed deuterium-tritium (DT) operation has become routine. The tritium delivery system provides considerable experimental flexibility, allowing individual beam sources to switch between D and T operation between shots. This allows convenient comparison between DT shots and reference shots with only D injection (D shots).

The tritium system has evolved significantly (Anderson 1994). Several hundred "line breaks" have been performed, where tritium-containing volumes have been decontaminated and opened for repair or maintenance activities. To date, over 400 kCi of tritium have been processed. Most of this never enters the torus and is trapped on the neutral beam cryopanels. These are periodically regenerated, allowing the gas to be processed. A tritium purification system, which will allow for onsite recycling of tritium is the in final stages of testing. Careful accounting of tritium usage indicates that roughly 2% of the input is held up in the torus and associated piping, representing a retention fraction of ~50% of the amount injected into the torus.

Machine activation has not prevented critical repair and maintenance activities. One week after high power DT operation, the radiation level near the vacuum vessel is in the range of 150 mrem/hr (1.5mSv/hr). However, careful planning has allowed repairs, for example, of vacuum vessel leaks, coil coolant leaks, and diagnostic actuators all of which are near the machine. Diagnostic calibrations continue to be performed. Neutral beam source replacements occur periodically. Since the activation is dominated by components with a half life of a few years, the activation for continued operation at current neutron production rates will increase only 20-30%/year, allowing for continued access for these activities.

3. Maximizing Fusion Power Production

Neutral beam heating and fueling has been the most effective means for reaching high fusion reactivity on TFTR. Twelve beam sources inject almost tangent to the plasma, with half injecting along the direction of the plasma current and half counter to the current direction. Up to 39.5 MW of neutral beam injection (NBI) has been achieved using 7 T and 5 D sources. The plasma configurations for the DT experiments have varied within 2.45 m < R < 2.62 m, 0.80 m < a < 0.97 m, 4.6 T < B_T < 5.6 T, and 0.6 MA < I_p < 2.7 MA. The primary limiter has been the toroidal inner carbon limiter.

Maximum performance has been produced in the hot ion or supershot mode of operation, characterized by $T_i(0)$ = 20 - 45 keV, $T_e(0)$ = 10 - 14 keV, highly peaked density profiles with $n_e(0)/\langle n_e \rangle$ = 2 - 4.5 and confinement enhancement up to H=2.4 (x ITER89P). High confinement in this mode is correlated with low edge influxes of H, D, and C, causing the core fueling to be dominated by the beams. For DT experiments, this allows for some control over the D:T species mix in the core, for example, to obtain the optimum 50:50 fuel mixture, or to study the isotope scaling of confinement.

The highest confinement and lowest edge influx has been reached by conditioning the limiter with Li pellets (Mansfield 1995), injected in the ohmic phase preceding NBI. Up to 4 pellets per shot can be injected at 0.4 - 0.6 km/s, each pellet containing 4×10^{20} atoms. Thus far the confinement in these discharges improves, up to the stability limit, with the number of Li pellets used, allowing considerable flexibility in optimization.

The effectiveness of Li wall conditioning, particularly at high input power is illustrated in Figure 1, which shows the fusion power production as a function of heating power for a large number of DT discharges with an optimal D:T mix. Peak fusion performance at a given power is produced with the aid of multiple Li pellet injection into the target ohmic plasma. The parameters for two such discharges, described below, are shown in Table 1.

Over the last year, the machine capability was extended in several areas to achieve the highest fusion power discharge (80539) with P_{fus} = 10.7 MW (McGuire 1995). More aggressive use of Li pellet conditioning to reduce wall influxes permitted the achievement of supershot performance at plasma currents up to 2.7 MA. In addition, the toroidal field has been increased from 5.1 to 5.6 T. With DT operation on TFTR, the fusion power was found to scale empirically as $P_{fus} \propto W_{tot}^{1.8}$ (Strachan 1994). At the Troyon-like supershot stability limit $W_{tot} \propto I_p \cdot B_T$. Hence, incremental improvements are significant in boosting fusion output. It should be noted that the performance on shot 80539 was limited by a minor disruption, and that additional confinement enhancement through the use of more Li was possible.

Characterization of the stability limit for high performance supershots is discussed in a later section.

An example of the effectiveness of more aggressive Li conditioning is shot 83546, which attained the record value $n_{hyd}(0)\tau_E^*T_i(0) = 8.7x10^{20}$ m^{-3}·sec·keV at only 17 MW of injected power (where n_{hyd} is the total hydrogenic density and $\tau_E^* = W_{tot}/P_{tot}$). In addition to the use of 4 pellets in the ohmic target, in this case multiple pellets were injected into several preceding ohmic discharges, resulting in extremely low edge influxes. This discharge disrupted, after achieving a confinement time $\tau_E = 0.33$ sec.

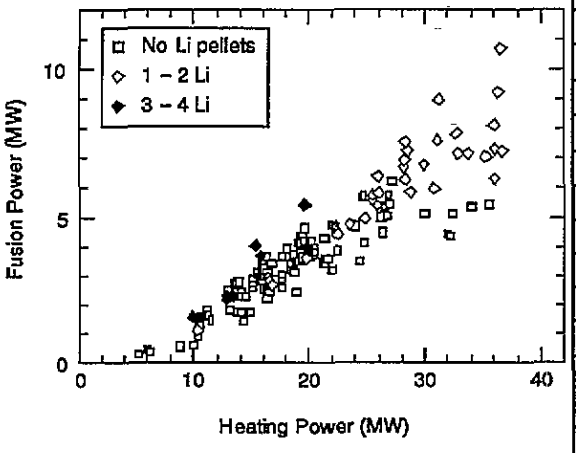

Figure 1. Dependence of peak DT fusion power on total heating power (NBI + ohmic).

shot	8059	8356
I_p (MA)	2.7	2.3
B_T (T)	5.5	5.5
P_{inj}(MW) D	14.2	0.0
P_{inj}(MW) T	25.3	17.0
$n_e(0)$ (10^{19}m^{-3})	10.0	8.5
$n_e(0)/\langle n_e\rangle$	2.7	4.5
n_{hyd} (10^{19}m^{-3})	7.4	7.0
v_Φ (10^5 m s^{-1})	1.3	6.5
$T_i(0)$ (keV)	32	44
$T_e(0)$ (keV)	13.5	12.3
Z_{eff}	2.4	1.9
W_{tot} (MJ)	6.9	4.9
τ_E (sec)	0.21	0.33
H (ITER89P)	2.1	2.4
β_N	1.8	1.3
P_{fus} (MW)	10.7	3.0
# Li pellets	2	4
$n_{hyd}\tau_E^*T_i(10^{20})$	4.1	8.7

Table 1

4. ICRF Heating and Current Drive

Effective fast wave ICRF heating of majority ions in D-T plasma at $2\Omega_T$ is an important scenario for ITER and has been demonstrated in TFTR supershots. The scenario involved combined ICRF and NBI heating with 23.5 MW and 5.5 MW, respectively. A 2% ^{3}He minority was present and 60% of the beam fueling was tritium. The central ion temperature rose during ICRF from 26 - 36 keV, consistent with 2D code predictions. $T_e(0)$ increased from 8.5 - 10.5 keV, due to direct electron damping and ^{3}He tail heating (Taylor 1994).

To characterize power absorption in this heating regime, the response of T_e and T_i to RF modulation at 10 Hz was studied as the tritium fraction (6%-40%) and resonance location were varied. Typically 50-70% of the RF power is deposited on the ions and 20-30% on electrons, in rough agreement with modeling expectations (Phillips 1995).

As suggested by Majeski, mode conversion of the fast magnetosonic wave into the ion Bernstein wave can be used to provide on and off-axis electron heating and current drive in mixed species plasmas (Majeski 1994). To date,

D-^{3}He and D-T-^{3}He plasmas have been used, with DT experiments planned for upcoming operation at B_T = 6.0 T. Using this technique, $T_e(0)$ has been raised from 3 - 10 keV with 4.4 MW of centrally deposited power. This technique has also been used to drive 125 kA on-axis with 2 MW, and 100 kA off-axis with 4 MW of RF power (Majeski 1995a, b).

Strong, phase dependent coupling has been observed between the mode converted IBW wave and fusion tritons, causing a triton loss rate comparable to the birth rate (Darrow 1995). Furthermore, the escaping tritons were measured to have been heated by roughly 0.5 MeV. Understanding of such wave-particle interactions may foster the development of a means of channeling alpha energy to thermal ions rather than electrons, with a large gain in efficiency in the reactor concept (Fisch 1992).

5. Transport and Confinement

5.1. Tritium Particle Transport

Tritium transport on TFTR has been studied by puffing small amounts of tritium gas into a deuterium neutral beam heated discharge (Efthimion 1995). Neutron collimator measurements of the evolution of the neutron source profile, combined with perturbative transport techniques, provide a unique determination of hydrogenic ion transport coefficients. Consistent with earlier perturbative studies on TFTR, one finds that $D_T \approx \chi_D \approx D_{He}$, suggestive of transport due to electrostatic microinstabilities.

Tritium influx from the limiter has been measured with a Fabry-Perot interferometer which derives T_α intensities by comparing detailed spectral line profiles of H_α:D_α:T_α for tritium beam fueled discharges with comparable deuterium fueled reference cases (Skinner 1995). These are interpreted to indicate the relative edge concentrations of these species. Deuterium dominates the wall inventory due to the large number of beam and plasma setup shots in deuterium for every shot using tritium. Even on shots with all T neutral injection, values for $T_\alpha/(H_\alpha+D_\alpha+T_\alpha)$ are typically 2-5%. The H_α fraction is typically ~18%.

5.2. Isotope Scaling in DT Supershots

Relative to equivalent D-only discharges, confinement is clearly increased in supershot discharges with significant amounts of tritium fueling. In order to maximize the isotopic differences, matched sets of discharges with all T or all D injection are compared (Scott 1995). In the T-NBI plasmas, $T_i(0)$ is typically 25% higher, $T_e(0)$ is 5-10% higher, and $n_e(0)$ is ~10% lower for matched target plasma conditions. The stored energy and global confinement time are typically 25% higher for the T-NBI cases and 65-80% of this increase is due to an increase in the ion and electron thermal stored energy. The strongest effect is seen on the total effective ion diffusivity (including convection) χ_i^{tot}, which drops a factor of two between $0.1 \le r/a \le 0.7$. The momentum diffusivity χ_Φ^{tot}, and electron particle diffusivity D_e, drop by ~50% over this region, and the change in the electron thermal diffusivity χ_e^{tot}, is smaller and less certain.

Figure 2 shows the dependence of global τ_E and χ_i^{tot} on average ion mass, here defined as the average mass of the thermal hydrogenic ions <A>, within r/a=0.5, a volume containing more than 3/4 of the thermal stored energy.

Previous studies (Meade 1990) showed that χ_i^{tot} varied roughly as $1/T_i$ for supershot plasmas. By comparing T-NBI shots with D-NBI shots at slightly higher power, one finds that a strong isotope scaling persists even when evaluated at fixed local parameters $\chi_i^{tot} \alpha \langle A \rangle^{-1.8 \pm .02}$. This isotopic scaling in supershot (D/T) plasmas is much stronger than previously observed in L-mode (H/D) studies. It is hoped that future experiments can address isotope scaling in L-mode (D/T) plasmas.

Density fluctuation measurements were performed with a correlation reflectometer on several matched sets of D-NBI and T-NBI shots (Mazzucato 1995). In both cases at values of r/a of 0.3 and 0.5, the ratio of fluctuation amplitudes was 1 ± 0.2, in regions where the ratio of χ_i^{tot} values was ~ 2. Beam emission spectroscopy (BES) measurements of the ratio of density fluctuation amplitudes for similar D- and T-NBI shots in the region $0.6 \leq r/a \leq 0.75$ (Paul 1995) indicate a ratio of 2 ± 0.5, with lower levels in the T-NBI case. Both diagnostics measure the correlation length of the density fluctuations to be unchanged between D-NBI and T-NBI matched sets.

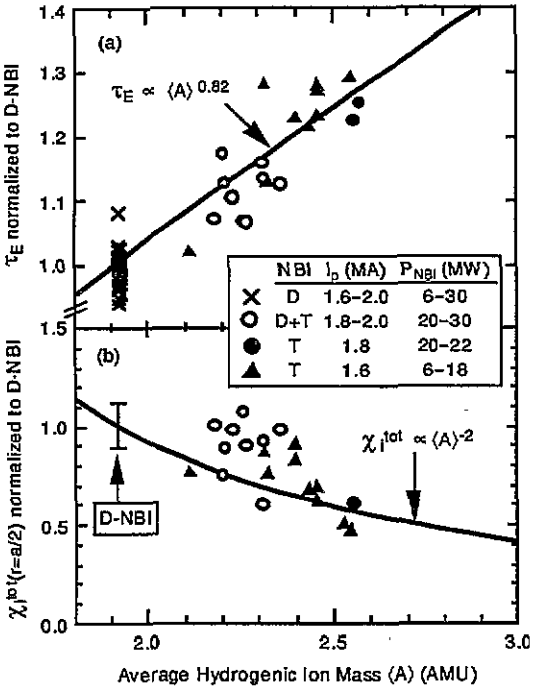

Figure 2. Variation of (a) global energy confinement and (b) total ion thermal diffusivity as a function of $\langle A \rangle$, the mean hydrogenic ion mass within r=a/2.

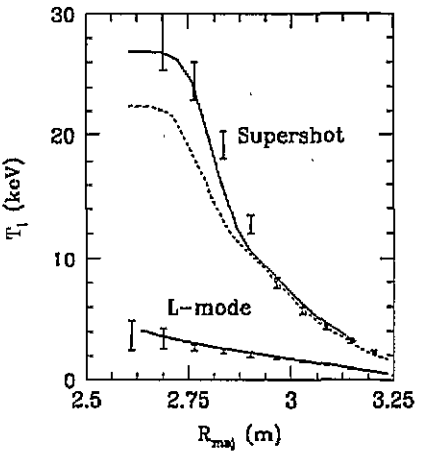

Figure 3. Predictions of the IFS - PPPL transport model. The top curve in the supershot case corresponds to a Z_{eff} profile which varies from central values of 2.5 to edge values of 4, and in the lower dashed curve the variation is from 2 to 5.

5.3. IFS-PPPL Model of Anomalous Thermal Transport

A model based on nonlinear gyrofluid simulations of ion-temperature-gradient driven (ITG) turbulence has recently achieved quantitative success in describing TFTR L-mode results, and provides potential explanations for the confinement enhancements in supershots (Kotschenreuther 1995). A

collaborative effort between IFS and PPPL, this model interpolates between an array of nonlinear simulations to arrive at a formulation for χ_i and χ_e. These have been used successfully to predict both the absolute magnitudes and the scaling trends of the transport coefficients and the temperatures for a database of TFTR L-mode discharges with widely varying parameters. In comparing with experiment, the model uses the measured density and radiation profiles, and the q and power deposition profiles inferred from TRANSP. Temperatures at r/a = 0.8 are then used as boundary conditions in calculating $T_e(r)$ and $T_i(r)$ in the core. Figure 3 shows the result for an L-mode and a supershot with the same heating power, line averaged density, current and toroidal field along with the measured profiles for these shots. The model qualitatively reproduces the large difference in T_i in these regimes. The model currently neglects trapped electron modes and rotation shear which are not important in L-modes but may be significant in supershots. Nonetheless, the model points to the stabilizing influence at the plasma edge of high T_i/T_e and modest deuterium dilution as possible causes for enhanced confinement in TFTR supershots.

A possible explanation of the isotope scaling is the sensitive dependence of the ITG stability threshold to the rotation profile or to the impurity profile. For example, Figure 3 shows the sensitivity to the assumed Z_{eff} profile. Moderate carbon concentrations tend to be more stabilizing for the ITG mode for tritium plasmas than for deuterium plasmas. However, detailed investigation of this hypothesis remains to be carried out. The ITG instability tends to be less sensitive to such secondary effects in L-mode plasmas, and an isotope scaling study in TFTR L-mode plasmas should provide a more definitive test of these theories.

6. Alpha Particle Physics

A primary goal of the TFTR DT program is the study of alpha particles. An array of alpha particle diagnostics has begun to characterize alpha confinement. In addition, considerable effort has been devoted to study the collective alpha effects on TAE instabilities, and evidence for alpha drive has been found. Some indications of alpha heating of electrons have also been observed.

6.1. Escaping Alpha Particle Measurements

An array of scintillator probes at various angles at the bottom of TFTR (ion ∇B drift direction) detect escaping alphas and other fusion products with pitch angle and gyroradius resolution. For the probe 90° below the midplane, the measured loss is consistent with expected single particle, first orbit loss for alphas in its dependence on plasma current, pitch angle, gyroradius and time (Zweben, 1995). Within the calibration uncertainty (a factor of 2), this first orbit loss is consistent with local predictions of the model. The model predicts that at I_p = 2.5 MA, the global first orbit loss is about 3%. The measured first orbit loss fraction does not increase with fusion power, further indicating that it is a single particle effect. Modeling of the losses to the probe 20° from the midplane is more complex and incomplete. It is expected that TF ripple diffusion plays a large role. Experiments are now planned to test the modeling, in particular, its dependence on q and q' through the use of current ramps.

As was the case for D plasmas, enhanced (over first orbit loss) alpha loss is seen to accompany MHD activity in DT plasmas. These enhancements are comparable in amplitude to the first orbit losses. Possibly resonant MHD-alpha particle effects have recently been observed in DT supershots at frequencies corresponding to the precession frequency of fattest banana orbits (~140 kHz). Alpha losses are observed to correlate with moderate-n kinetic balooning mode-like activity in the region of maximum pressure gradient. The role of alpha drive in this activity, if any, is not yet understood.

Losses up to 100 times the first orbit loss are sometimes seen just before the current quench of minor and major disruptions. Depending on the spatial localization of such losses, they could pose a serious hazard to the ITER first wall. Losses attributable to collective alpha driven instabilities have not been observed.

Alpha losses comparable to first orbit losses have been observed during ICRF fast wave heating of DT plasmas. Losses appear near the pitch angles corresponding to the fattest banana orbit. This indicates that alphas on marginally passing orbits are resonating with the RF and gaining perpendicular energy, which places them on lost orbits. A broadened gyroradius distribution for these losses also indicates that the alphas are being heated by the ICRF.

6.2. Confined Alpha Measurements

The pellet charge exchange (PCX) diagnostic has been used to study the energy and spatial distribution of the confined alphas and the effects of sawtooth activity. This diagnostic performs high energy neutral particle analysis of alphas neutralized in the ablation cloud of an injected Li or B pellet, yielding energy resolved radial profiles of the alpha distribution from 0.5 - 3.5 MeV at a single time in the discharge for near perpendicular pitch angles (Fischer 1995). To achieve sufficient pellet penetration, this diagnostic is presently constrained to make measurements after neutral beam injection, and it is not absolutely calibrated. In the core of sawtooth free discharges, the shape of the measured PCX energy spectrum agrees well with TRANSP modeling, assuming alphas are well confined and slow down classically. The measured ratio between detected intensities of alphas and tritons from a comparable D shot also agree with modeling. To be consistent with profile shape measurements away from the core, the model must include the effects of stochastic ripple diffusion. Recent measurements with the pellet injected 20 ms after a 0.1 sec 20 MW DT shot indicate a peaked energy distribution centered at ~2.5 MeV, with a width of ~ 30 keV, in reasonable agreement with model predictions (Medley 1995). Comparison of measurements in the presence and absence of sawteeth in the period following the DT heating phase indicate that the sawtooth transports trapped fast alphas radially outward, as shown in Figure 4. In these sawtooth cases, there is no enhanced alpha loss observed on the edge scintillator probes. However, the probes view a range in pitch angles which does not include the narrow range observed by the PCX diagnostic.

Line emission from charge exchange recombination of alphas with neutral beam atoms is used by the α-CHERS diagnostic to study alphas from mainly parallel pitch angles with $E_\alpha < 0.7$ MeV (McKee, 1995). This emission produces a feature on the long wavelength side of the thermal 4686Å line that is ~ 0.1% of the bremsstrahlung background, and analysis requires careful extraction of weak edge impurity lines and normalization and subtraction of the signal from a similar D reference discharge.

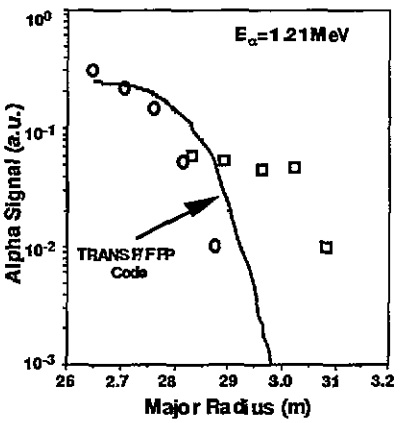

Figure 4. Spatial profile of the alpha signal at $E_\alpha = 1.2$ MeV before (circles) and after (squares) sawtooth activity.

The result is an absolutely calibrated fast alpha signal which can be studied with a time resolution of 100 msec at five spatial locations. Because of the effects of radiation-induced fiber fluorescence, measurements with this diagnostic are thus far limited to a D-only diagnostic phase following the main DT heating phase. The measured spectrum agrees with TRANSP predictions both in the absolute intensities and the spectral dependence (ie. alpha particle energy dependence), assuming classical collisional slowing down as calculated by TRANSP. Preliminary measurements of the spatial profile are being compared with this TRANSP model. For sawtoothing discharges, a decrease in core alpha density is observed.

6.3. Alpha Ash Measurements

Helium ash measurements have been made using charge exchange recombination spectroscopy of the n = 4 - 3, 4686Å line of singly ionized helium (Synakowski, 1995). In the experiment, an alpha population was established in a 1.25 sec heating phase of 21 MW of DT injection, then the T beams were turned off for .75 sec of D-only injection. Comparing line brightness during the final phase with a shot with comparable power waveform of D-only injection, one sees a clear enhancement due to the presence of the thermalized alpha ash. These measurements provide the spatial profile and the time evolution of the absolute ash density. Alpha ash does not peak strongly on axis, implying rapid transport with $\tau_{He}^* \sim 1.2$ sec, consistent with previous helium gas puff measurements of D_{He} and v_{He} (Synakowski, 1993). The time evolution is consistent with TRANSP modeling assuming classical alpha thermalization and assuming some wall pumping, $R_{He} \sim .85$. With comparable τ_{He}^*/τ_E and efficient edge pumping, ash accumulation should not be a problem for ITER.

6.4. ICE Measurements

Suprathermal ion cyclotron emission at multiples of the alpha cyclotron frequency at the outer midplane is observed by rf probes in supershots during the first 200 msec of DT beam injection (Cauffman, 1995). The characteristics of this emission are consistent with drive due to the magneto-acoustic cyclotron instability (Gorelenkov 1995, McClements 1995). The growth rate for this instability is enhanced by the initial narrow pitch angle distribution expected initially for alphas at the outside edge. Growth rates are also enhanced if the edge densities are high enough for the alphas to be super-Alfvenic, consistent with the observation that a helium gas puff

introduced late in the DT heating phase causes the emission to reappear. This is also the case when this emission is observed for JET H-modes (Cottrell 1993). Fortunately, this instability is localized to the outer edge and does not significantly affect alpha confinement.

6.4. The Effect of Alpha Particles on TAE Mode Activity

A low amplitude ($\delta B/B < 10^{-7}$), high frequency ($f \sim f_{Alfven}$), edge mode is routinely observed with the Mirnov system in both D and DT discharges. The amplitude of this Alfven Frequency Mode (AFM) was sometimes enhanced during high power DT shots, suggesting possible alpha drive. This activity was never seen on the reflectometer system probing the core. Furthermore, the frequency of this mode corresponds to the edge Alfven frequency at R=180 cm. Correlating the time evolution of observed changes in the frequency of this mode with that of edge density (due to ELMs, gas puffs, pellets, etc.), has clearly localized the mode at the plasma edge (Chang Z 1995). The driving mechanism for the AFM, which has been observed even in discharges with only ohmic heating, is certainly not alpha particles and has not yet been identified.

Toroidal Alfven eigenmodes (TAE) have been observed on TFTR (Wong 1994) and many other tokamaks driven by fast ion populations consisting of beam ions (in low B_T experiments) or H-minority ICRF tail ions. On TFTR, the presence of these modes is clearly seen in Mirnov coil data, which provides the frequency spectrum as well as the toroidal mode identification. Core localization is characterized by reflectometer data which provides the frequency spectrum and amplitude of core density fluctuations. Thus far with central β_α values up to .0035, no alpha driven TAE activity has been observed in normal DT supershots (with sensitivities of edge $\delta B/B > 10^{-9}$ for the Mirnov system and core $\delta n/n > 10^{-5}$ for the reflectometer system). This is consistent with predictions for several supershots with the global kinetic/MHD stability code Nova-K (Fu, 1995). Beam ion Landau damping and radiative damping due to the parallel electric field are the main damping mechanisms. For normal supershot profiles, an increase in the $\beta_\alpha(0)$ by a factor of ~3-4 is needed, according to NOVA-K predictions, to drive the TAE unstable.

Attempts have been made to optimize conditions for destabilization of TAE modes. Increasing q(0) enhances the coupling to the alphas by moving the radial location of the TAE gaps inward toward the region of maximum alpha pressure gradient (Batha 1995). Transiently lowering T_i with pellets and gas puffs should have reduced the ion damping terms (Zweben 1995). To date, these efforts have failed to result in alpha driven TAE instability, consistent with NOVA-K predictions.

As a way of probing for the presence of alpha drive, the H-minority ICRF power threshold necessary to drive TAE activity was studied in D and DT supershots where the plasma parameters, and hence the damping rates, are comparable (Wong 1995). Figure 5 shows the TAE amplitude, integrated over the closely spaced peaks in the Mirnov spectrum observed as the power threshold for the TAE instability is 20% lower in DT plasmas compared with similar D shots. Modeling using the FPP code and TRANSP indicates nearly identical RF power deposition (70%) to H-minority ions, and hence D and DT shots with the same power should have the same RF drive for the

instability. Fast neutral charge exchange measurements confirm that the H-tail temperatures are the same in the two cases at the same RF power. Damping due to fast beam ions is also predicted to be nearly identical in the two cases. According to analysis with the NOVA-K code(Cheng C Z 1991), at 5.3 MW RF power and 3 MW fusion power, the ratio of the growth rates $\gamma_\alpha/\gamma_{H\text{-min}} \sim 10\%$. These observations and analysis suggest that the reduced power threshold in the DT plasmas is due to the alpha particles.

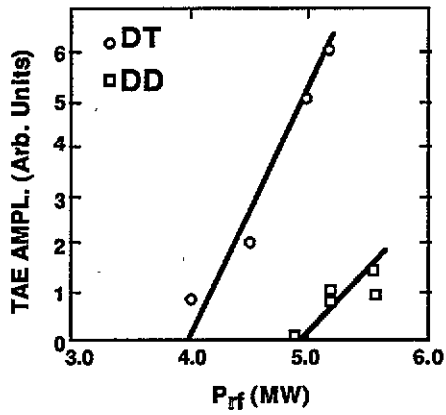

Figure 5. Integrated Mirnov mode amplitude vs. RF power showing dependence of amplitude and power threshold on presence of alpha particles

Concern about TAE mode effects is well founded. RF-induced TAE mode activity, during a recent H-minority ICRF heating experiment, caused a large population of fast ions to become ripple trapped and lost (White 95). This resulted in localized heating and failure of two TFTR vacuum vessel welds. Avoidance of certain parameter ranges and spectroscopic monitoring for Mn (a high vapor pressure component of stainless steel) has prevented recurrence.

6.5. Indications of Alpha Heating of Electrons

Attempts to observe clear signs of alpha heating of electrons have been challenged by uncertainties in the beam dynamics, by the isotope effect, and by the inherent variations in the effects of MHD and conditioning on performance. Within r/a~0.25, the alphas are calculated to contribute up to 15% of the electron power flow during the DT heating phase. For comparable high performance supershots, TRANSP modeling of the steady state electron power balance indicates that roughly half of the 2 keV difference in the central electron temperature in D vs DT plasmas is due to alpha heating, assuming χ_e is unchanged.

The database of DT shots has grown to the point that there are now sufficient numbers of similar D, DT, and TT shots to study the electron temperature scaling in the heating phase of these supershots. Previous studies (Strachan 1992) have shown that for D discharges, $T_e(0)$ depends on B_T, the global confinement time τ_E, and the beam voltage W_B, with a weak dependence on beam directionality (Strachan 1993), and no significant dependence on heating power.

For more recent data, Figure 6 shows a comparison of the average electron temperature profile for an ensemble of similar DT shots and D shots with the same average confinement time and power. The comparison is done at the same confinement time to compensate for effects due to isotopic mix and conditioning. The DT shots are clearly hotter at a given confinement

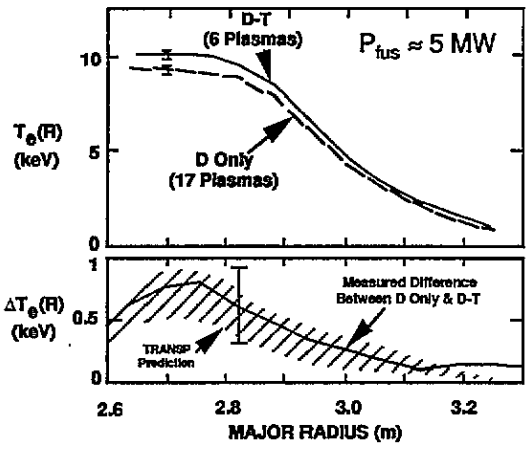

Figure 6. Dependence of central electron temperature on global confinement time for supershots with differing species mix showing enhanced central heating in presence of alpha particles.

time, suggestive of alpha heating. In addition, this $T_e(0)$ difference is consistent with TRANSP expectations of alpha heating in its absolute magnitude, its radial dependence, its time dependence, and its scaling with fusion power. More systematic experiments with closely matched parameters are planned to continue this work.

Suggestions of alpha heating are also seen in the time evolution of the electron temperature in high performance cases with extensive Li conditioning where the DT heating phase ends abruptly. Electron temperatures in a shot similar to 80546 in Table 1, that did not disrupt, reached record levels, T_e=14.8 keV, in this post-beam phase compared to 10.5 keV in similar D shots.

7. MHD Stability Limits and Performance

On TFTR both the achievable central plasma pressure and the time over which high pressure can be maintained is limited by MHD stability. With the gains in confinement obtained with aggressive Li conditioning of the limiter, TFTR has sufficient heating power available to push to enhanced stability limits. If a means could be found to increase the stability limit, the fusion power production as well as the possibilities for studying alpha heating and alpha driven instabilities would be increased greatly. Theoretical predictions indicate that reversed magnetic shear configurations, recently produced on TFTR, offer advantages, not only for confinement and stability, but also for bootstrap current alignment (Kessel 1994, Manickam 94). A similar configuration is being considered for the Tokamak Physics Experiment (TPX) (Goldston 1993).

7.1. Disruptions of High Performance Discharges on TFTR

The disruption threshold for normal TFTR supershots is illustrated in Figure 7, characterized in terms of $\beta_N=\beta_T aB_T/I_p$ and the density peakedness $n_e(0)/\langle n_e\rangle$. This figure does not include shots with current ramps. It is clear that as the peakedness increases, the achievable β_N decreases, and that the product of these parameters is a useful predictor for disruptions (Mueller 1995). These disruptions have no precursor occurring soon enough to allow for avoidance measures. Using a fast digital processor doing real time analysis of magnetic data to calculate β_N, a feedback system has been used successfully to control the beam power. Work is in progress to provide a real time measure of the density peakedness as well, in the hope of more aggressively pursuing studies safetly below the disruptive limit, to avoid extensive reconditioning of the machine following major disruptions.

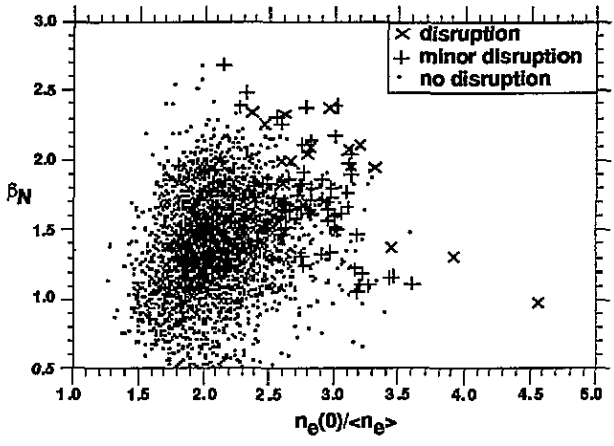

Figure 7. The normalized beta and density peakedness are plotted for a collection of plasmas to illustrate the stability threshold, currently the limit on supershot fusion performance

Stability beyond the limit described above has been demonstrated in high edge shear, current ramp-down plasmas (Sabbagh 1995). Up to 6.7 MW of fusion power, with β_N = 3.0, and $H \approx 3.1$ have been achieved in such a plasma at I_p=1.5 MA (ramped down from an initial value of 2.5 MA) and P_b = 31 MW. Peaking the current profile by ramping down the plasma current prior to the main heating phase has allowed fusion power performance comparable to normal supershots with the current maintained at the initial value. This demonstrates the potential for enhancing stability limits by current profile modification.

Often the disruptions which occur in high performance discharges begin with the fast onset (500 μsec) of an n=1 internal kink which couples to an external kink. These low-order-modes then appear to trigger high-mode-number, toroidally localized ballooning modes resulting in the disruption (Fredrickson 1995). According to stability analysis using measured current and pressure profiles with the PEST code (Manickam 1994), the observed β limit is consistent with the growth of low-mode-number internal and/or global instabilities. Calculations with PEST have shown that modification of the current profile can result in a substantial increase in the β limit for marginal stability of these modes. For example, the 10.7 MW DT shot (80539) suffered a minor disruption at $\beta_N \sim 1.8$. For the same shot with a hollow j(r) profile and a region of reversed shear, PEST predicts a stability limit of β_N = 2.7. Fusion power performance in DT on TFTR scales approximately as β_N^2. If the pressure profile could be maintained while the current profile was modified to enhance to stability limit to β_N=2.5 at I_p= 2.5 MA and B_T=5.5T, a fusion power of 17 MW is within reach.

7.2. Reversed Magnetic Shear Operation on TFTR

Reversed shear configurations have recently been produced on TFTR with interesting core confinement characteristics (Levinton 1995). One approach is illustrated in Figure 8a. The plasma is started at full size and the current is ramped up, forcing the current to form at the edge. Since the current diffusion time is slower than the rise time of the total plasma current, the j(r) profile is hollow during the ramp. A low power heating prelude phase heats the electrons from 2 to 5 keV, decreasing the plasma resistivity and slowing

the inward diffusion of current. This is followed by the main heating phase of up to 25 MW of beam injection.

Measurements of the q(r) profile with the Motional Stark Effect (MSE) diagnostic at the end of the current ramp and the end of the heating phase are shown in Figure 8c. Values for q(0) and q_{min} are observed to decrease monotonically with time through both phases, consistent with neoclassical current diffusion. With variations of beam timing and total current, a range of configurations have been produced, with q(0) in the range from 2 - 5 and q_{min} from 1.8 - 3.

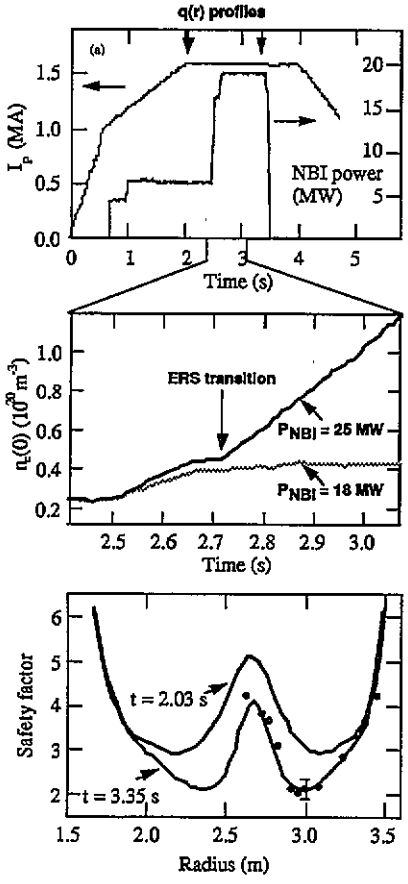

Figure 8. Time evolution (a) of the plasma current and NBI power for reversed shear scenario and expanded view, (b) showing central density and transition to R/S mode, and (c) the q profiles at two times.

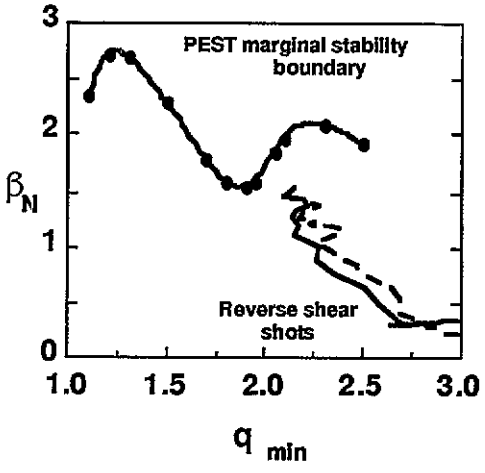

Figure 9. The top curve is the boundary for marginal stability calculated by PEST for the n = 1 infernal mode with wall at infinity. In the calculation, q(0) = q_{min} - 1, and the pressure profile is fixed.

The confinement characteristics of shots with less than P_{inj}~18 MW in the main heating phase resemble supershots with the same machine parameters. However, above a power threshold of ~ 18 - 20 MW, the core transport changes abruptly 0.2 - 0.3 sec into the main heating phase within the region of reversed shear. The effect is most clearly seen on the central

density evolution, shown in Figure 8b. The central density rises by more than a factor of 2 in 0.3 sec. Since the density outside the reversed shear region changes little, the density profile following the transition becomes very peaked, reaching values of $n_e(0)/\langle n_e \rangle \sim 4.2$. The core electron temperature increases by 25%, and the ion temperature profile broadens. At the transition, the inferred electron particle diffusivity drops by a factor of 50 to near neoclassical levels. On some shots the electron and ion thermal diffusivity drop by a factor of 2-3. The pressure gradient in this enhanced reversed shear (ERS) mode is larger, by a factor of 3-5, than typical supershots, which very often have low-n MHD modes in the core. In the region of reversed shear, MHD activity is absent in ERS discharges as measured by the 4 channel reflectometer. Unfortunately, high performance ERS shots have ended in a disruption shortly after the appearance of a low-n MHD mode just outside the q_{min} radius when $q_{min} \sim 2$. The cause for these disruptions is under investigation.

Figure 9 shows the trajectory of two R/S shots which ended in a disruption, superimposed on a plot of β_N vs q_{min} for marginal stability calculated by PEST. The calculation assumes a reversed shear q profile with $q(0) = q_{min} + 1$, and a fixed, peaked pressure profile. In order to reach higher β_N, q_{min} needs to further decreased. The challenge is to reduce q_{min} while maintaining a significant spatial extent for the reversed shear region.

Future work will continue to explore the potential for this new ERS regime in extending the stability limit, including operation in DT. If high performance in DT can be achieved, this would be a very interesting regime in which to study alpha driven TAE modes. Experiments will also include documentation of the core fluctuations, studies of the particle transport by T puffing, and He ash accumulation in DT ERS discharges.

Summary

Extensive operation with mixed DT plasmas on TFTR has yielded results which are encouraging for the DT reactor concept. There is a strong positive isotope scaling in high performance supershot plasmas. The ITER scenario using fast-wave ICRF heating of majority ions in D-T plasmas at $2\Omega_T$ has been demonstrated. Alpha particles behave as expected. They are well confined at high currents, and slow down classically. Alpha ash is rapidly transported out of the plasma. Initial indications of alpha heating have been observed. There is evidence for alpha drive as a contributor to RF-tail-driven TAE activity. However, consistent with modeling, alphas alone have not driven TAE modes, at levels of $R\nabla\beta_\alpha \sim 1/3$ that expected for ITER. With the use of Li wall conditioning, TFTR has adequate confinement and heating power to reach higher values of β_α, if enhanced MHD stability could be achieved. A new reversed shear configuration has been obtained with enhanced core confinement and the promise of improved stability.

Future Plans

Continued DT operation on TFTR is planned at least until September, 1995. A proposal for extending operation is under review. Based on the operating experience to date, TFTR can continue to operate safely and reliably with DT plasmas for several more years.

There are proposed experiments for continued characterization of alpha physics, both single particle and collective effects. An element of continued operation will be to pursue higher and more sustained fusion power performance, to foster these studies. This will entail a thorough investigation of techniques to improve MHD stabilility for supershots, by current or pressure profile modification. Isotopic mass scaling, ICRF $2\Omega_T$ heating experiments, and fluctuation measurements in L-mode plasmas are also planned, as well as mode conversion current drive studies in DT plasmas.

Acknowledgements

The authors express their appreciation to the PPPL technical, engineering, and scientific staffs for their efforts in the execution and interpretation of these experiments, to our collaborators for the tools and expertise they provided, and to Drs. R. C. Davidson and P. Rutherford for their support and encouragement. Work supported by U.S. Department of Energy Contract No. DE-AC02-76-CH0-3073

References

Anderson J L *et al* 1995 *Plasma Physics and Controlled Nuclear Fusion Research Seville 1994* (IAEA Vienna 1995)
Batha S H *et al* 1995 submitted for publication in *Nuclear Fusion*
Cauffman S *et al* 1995 submitted for publication in *Nuclear Fusion*
Cheng C Z 1991 *Phys. Fluids B* **3** 2463
Chang Z 1995 submitted to *Phys. Rev. Lett.*
Cottrell G *et al* 1993 *Nucl. Fus.* ***33*** 1365
Darrow D *et al* 1995 to appear in Proceedings of the 11th Topical Conference on Radiofrequency Power in Plasmas Palm Springs 1995 (American Physical Society)
Efthimion P *et al* 1995 *Plasma Physics and Controlled Nuclear Fusion Research Seville 1994* (IAEA Vienna 1995)
Fisch N and Rax J M 1992 *Phys. Rev. Lett.* **69** 612
Fischer R *et al* 1995 submitted to *Phys. Rev. Lett.*
Fonck R *et al* 1995 *Plasma Physics and Controlled Nuclear Fusion Research Seville 1994* (IAEA Vienna 1995)
Fredrickson E *et al* 1995 submitted to *Phys. Plasmas* (PPPL Report 3023)
Fu G *et al* 1995 submitted to *Phys. Rev. Lett.* (PPPL Report 3110).
Gorelenkov N N and Cheng C Z 1995 submitted for publication in *Nuclear Fusion*
Goldston R et al 1993 *Proc. 20th Euro. Conf. on Contr. Fusion and Plasma Phys.,Lisbon* 319
JET Team 1992 *Nuclear Fusion* **32** 187
Kessel C, Manikam J, Rewoldt G and Tang W M, 1994 *Phys. Rev. Lett.* **72** 1212
Kotschenreuther K, Dorland W, Beer M and Hammett G 1995 *Phys. Plasmas* **2** 2381
Levinton F 1995 submitted to *Phys. Rev. Lett.*
Manickam J *et al* 1994 *Phys. Plasmas* **1** 1601
Mansfield M *et al* 1995 *Proc. 22th Euro. Conf. on Contr. Fusion and Plasma Phys.,* Bournemouth
Majeski R, Phillips C K and Wilson J R 1994*Phys. Rev. Lett.* **73** 2204

Majeski R *et al* 1995a submitted to *Phys. Rev. Lett.*
Majeski R *et al* 1995b *Proc. 22th Euro. Conf. on Contr. Fusion and Plasma Phys.*, Bournemouth
Mazzucato E, Nazikian R and Scott S D 1995 *Proc. 22th Euro. Conf. on Contr. Fusion and Plasma Phys.*, Bournemouth
McClements K *et al* 1995 submitted for publication in *Phys. Plasmas*
McGuire *et al* 1995 *Phys. of Plasmas* **2** 2176
Meade D *et al* 1990 *Plasma Physics and Controlled Nuclear Fusion Research Washington DC 1990* (IAEA Vienna 1991)
Medley S *et al* 1995 *Proc. 22th Euro. Conf. on Contr. Fusion and Plasma Phys.*, Bournemouth.
McKee G 1995 submitted to *Phys. Rev. Lett.*
Mueller D *et al* 1995 submitted to *Fusion Technology*
Paul S *et al* 1995 *Proc. 22th Euro. Conf. on Contr. Fusion and Plasma Phys.*, Bournemouth
Phillips C *et al* 1995 *Phys. Plasmas* **2** 2427
Sabbagh S *et al* 1995 *Plasma Physics and Controlled Nuclear Fusion Research Seville 1994* (IAEA Vienna 1995)
Scott S D *et al* 1995 *Phys. Plasmas* **2** 2308
Skinner C H *et al* 1995 *Nuclear Fusion* **35** 143
Strachan J *et al* 1993 *Nuclear Fusion* **33** 991
Strachan J *et al* 1994 *Proc. 21st Euro. Conf. on Contr. Fusion and Plasma Phys.*, Montpellier
Synakowski E 1995 submitted to *Phys. Rev. Lett.*
Synakowski E *et al* 1993 *Phys. Fluids B* **5** 2215
Taylor G *et al* 1995 *Plasma Physics and Controlled Nuclear Fusion Research Seville 1994* (IAEA Vienna 1995)
White R *et al* 1995 *Phys. Plasmas* **2** 1
Wong K L *et al* 1991 *Phys. Rev. Lett.* **66** 1874
Wong K L *et al* 1994 *Plasma Phy. and Control. Fusion* **36** 879
Wong K L *et al* 1995 submitted to *Phys. Rev. Lett.*
Zweben S 1995 submitted to *Nuclear Fusion*